Quantifying Vertical Differences in Green Visibility in High-Density Cities: A Voxel-Based Analysis Method

Haoyu Wang [1], Liu Liu [1], Sisi Zlatanova [2]

[1] Department of Urban Planning, College of Architecture and Urban Planning, Tongji University, Shanghai 200092, China - 2053245 @tongji.edu.cn; l.liu@tongji.edu.cn
[2] UNSW Built Environment, Red Centre Building, Kensington NSW 2052, Sydney, Australia - s.zlatanova@unsw.edu.au

Keywords: Voxel, Vertical Green Visibility, Spatial Openness, Airborne LiDAR, High-rise Green Exposure.

Abstract

Urban green spaces are important for residents’ physical and mental health, but green visibility is difficult to quantify in high-rise, high-density cities, especially across different height levels. To address this problem, this study proposes a stratified green visibility framework based on airborne LiDAR point clouds and a voxel model. Using the Dutch AHN5 dataset, the study area was converted into a unified 3D voxel space and classified into trees, grass, buildings, ground, and empty space. A voxel-level penetration probability model based on the Beer–Lambert law was introduced to represent the semi-transparent blocking effect of tree canopies, improving upon conventional binary visibility models. Multi-directional line-of-sight (LOS) tracing was then applied to calculate green visibility (GVI) and spatial openness (SOP) at different height layers. The results show that GVI is generally high around parks, large green spaces, and some enclosed courtyards, but its contribution from street trees is limited. Vertically, GVI decreases with height, while SOP tends to increase. Combining the two indicators helps identify different spatial types with distinct visual characteristics. The study demonstrates that airborne LiDAR, combined with voxelization and probabilistic 3D simulation, can effectively capture the vertical variation of urban GVI and support large-area assessment in high-density residential environments.

1. Introduction

Urban green space quantity and quality confer measurable benefits to residents’ physical and mental health (Feng and Yang, 2023, Jia et al., 2023, Li et al., 2025). However, the rapid urbanization experienced in many developing countries has led to extensive emergence of high-rise, high-density residential neighbourhoods. This urban form not only reduces the feasibility of indoor green visibility, but may also create vertical differences in green visibility and even intensify spatial inequality in residential environments. At the same time, the trend toward finer and smarter urban governance has increased the demand for analytical methods that are both effective and broadly compatible with city-scale datasets which are often constrained in accuracy (Wang et al., 2024).

Existing studies that rely on ground-level panoramas (Kumakoshi et al., 2020; Wu et al., 2021) or high-precision UAV photogrammetry (Xia et al., 2023) usually reflect results from only a limited number of viewpoints, or require excessive effort for data collection, which limits scalability. Even at the three-dimensional scale, studies using white models still face the problem of failing to realistically represent the characteristics of trees (Yu et al., 2016), or convert the analysis back into two-dimensional images during the computation stage (Tang et al., 2023). Although various methods have been proposed, there is still a lack of a city-scale analytical framework suitable for high-rise and high-density environments that can use medium-precision airborne point clouds and simulate the semi-transparent occlusion effects of vegetation under true 3D conditions.

To fill this gap, this study focuses on the vertical differences in green visibility and proposes a true 3D calculation framework. From a human-centered perspective, the framework aims to compute vertically stratified green visibility using point cloud data of limited precision. We use 3D grid, *i.e.,* voxels as the basic unit and integrate lightly semantically labelled point cloud information from the AHN5 airborne LiDAR dataset (AHN, 2023) into a unified model. The voxel types and point cloud semantics not only maintain spatial semantic consistency, but also support cross-height comparison and analysis of green visibility. On this basis, we introduce a voxel-level penetration probability model to simulate the effect of partial semi-transparent tree canopies on line-of-sight (LOS) transmission. This provides a solution to the limitations of traditional image-based methods, which cannot realistically simulate vegetation occlusion and visual penetration distance.

2. Methods

At present, many studies use the Green View Index (GVI) to measure green visibility. GVI represents the degree to which a person standing at a certain location can see green plants or vegetation (Yang et al., 2009). A number of researchers have calculated GVI in different studies using various methods, such as calculating the proportion of green pixels from Google Street View images (Ki and Lee, 2021), or generating panoramic views from LiDAR data at a given viewpoint to calculate the proportion of vegetation point clouds (Tang et al., 2023). However, many studies pay more attention to data representation than to people’s actual perception. Quantifying the sensory function of urban green space is not easy, for it is difficult to analyse three-dimensional morphology and vegetation distribution from a human perspective (Yu et al., 2016, Wang et al., 2021).

This study introduces a penetration probability model based on the Beer–Lambert law (Casasanta et al., 2022) to simulate the process by which a person’s LOS passes through leaves of different sparsity levels. This process involves intensity attenuation caused by leaf density and ultimately affects the green visibility scores. The proposed method consists of three main parts, and the overall workflow is shown in Figure 1:

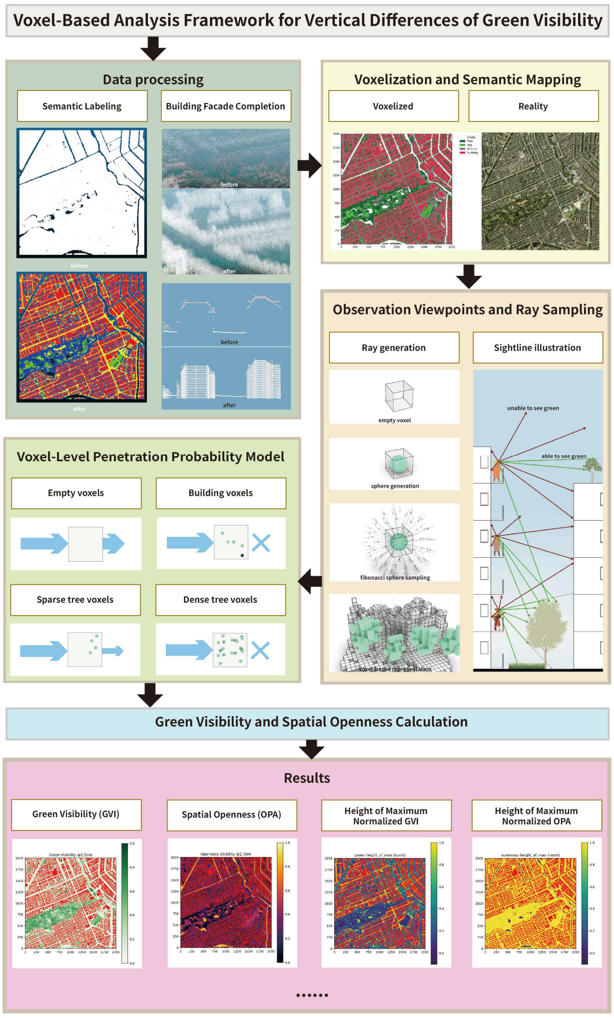

Figure 1. Overall workflow of the proposed method.

This study extends the core concept of GVI, where the GVI defined here is no longer equivalent to the traditional GVI based on the proportion of green pixels in images. Instead, it is a 3D green visibility indicator based on voxel LOS tracing and probabilistic attenuation (Aleksandrov et al., 2019). Specifically, we define green visibility (*GVI*) as follows: From the position of a given voxel, a certain number of rays are generated and cast in all directions in the form of a visual window to represent LOS. Based on the green visibility encountered along the path of each LOS, the green visibility score of each LOS within the viewing distance is calculated, and the average score of all LOS is regarded as the *GVI* of that place.

This study also combines penetration probability with the concept of *spatial openness* （*SOP*）, which is defined as follows: From the position of a given voxel, a certain number of rays are generated and cast in all directions in the form of a visual window to represent LOS. According to the semantic type and distribution density of voxels along the path, the attenuation of LOS intensity is calculated, and the remaining intensity of each LOS within the viewing distance is accumulated to obtain the penetration distance in that direction. The average penetration distance of all LOS is then taken as the *SOP* of that place.

2.1 Data Source and Processing

Urban landscape open spaces belong to small-scale spatial units, and traditional terrain data are difficult to quantify their fine morphological characteristics accurately, whereas LiDAR point clouds can provide high-precision 3D spatial information (Wang et al., 2021).

This study uses the publicly available AHN5 point cloud dataset (AHN, 2023), which has already undergone partial preprocessing and has been divided into square tiles of 1 km side length. Amsterdam’s city centre contains a large number of high-density residential areas, making it suitable as the experimental area for our calculation method. Therefore, we selected a 2 km × 2 km area with relatively high building density in the city centre, covering four files.

Although the dataset does not provide detailed semantic labelling, semantic labelling methods have already been sufficiently developed and available (Aljumaily et al., 2023; Huang et al., 2022; Zhang et al., 2023). As the preprocessing step, it is not the focus of our experiment. Therefore, with reference to the official documentation, we manually conducted lightweight semantic labelling of the point clouds. The point clouds were divided into four categories: *trees, grass, buildings*, and *ground*. This classification can meet the needs of our experiment while adapting to the characteristics of the dataset, and it is convenient to implement with limited processing of the original data. The selected study area and the classified results are shown in Figures 2 and 3.

Due to the characteristics of airborne point cloud scanning, many building facades are incomplete. These incomplete facades could seriously affect our experiment, because these areas that should not be penetrable would be identified as transparent. To address this problem, after the classification of point clouds, we translate the building roofs downward at 1 m intervals until the entire building is covered. With extremely low computational cost, this preprocessing step ensures the topological completeness of building boundaries in the following LOS tracing computational process and avoids GVI errors caused by LOS leakage. The differences before and after the process are shown in Figure 4.

Figure 2. Study area in Amsterdam.

This contribution has been peer-reviewed.
https://doi.org/10.5194/isprs-archives-XLIX-B4-2026-529-2026

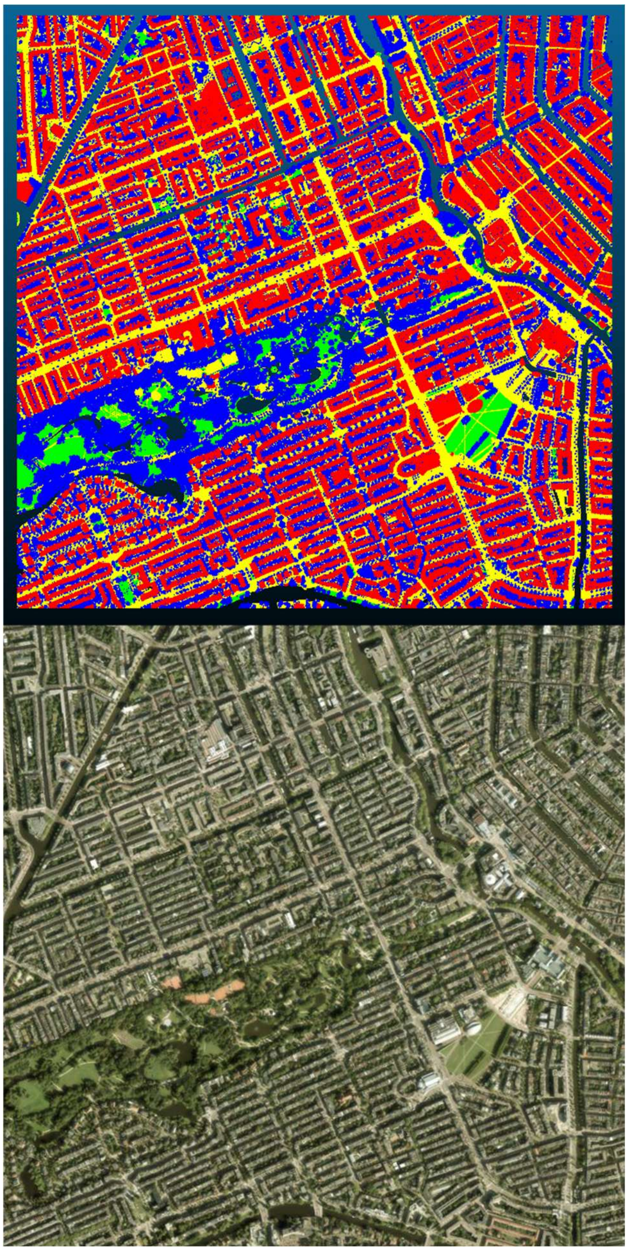

Figure 3. Point cloud and corresponding real-world scene.

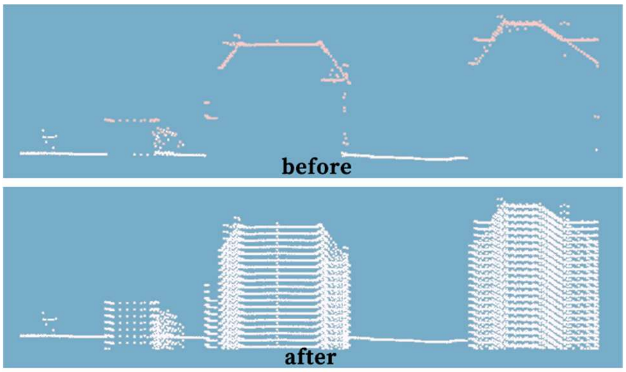

(a)Building completion shown in 2d

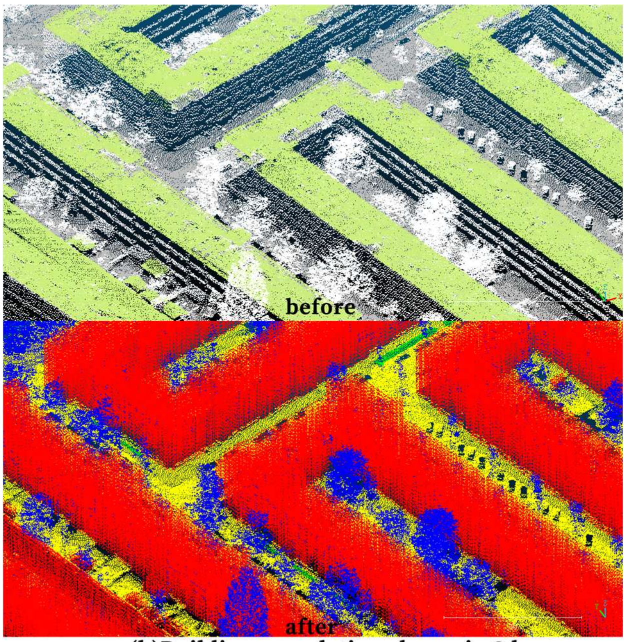

(b)Building completion shown in 3d

Figure 4. Building completion before and after preprocessing. (a) shows the comparison in 2d, (b) shows in 3d, green represents buildings before the process, and red after the process.

2.2 Voxelization and Semantic Mapping

Voxel is the extension of a two-dimensional grid into three-dimensional space and is an important form for converting point cloud data into structured 3D data (Xu et al., 2021). The voxelization process is applied before GVI computation. The voxel size is an adjustable parameter that can be determined through preliminary experiments. Based on the characteristics of the dataset and the results of preliminary tests, we confirm that a side length of 1m is suitable for the precision required in this study while not placing excessive demands on computational cost. Therefore, the study area was voxelized with the resolution of 1m.

In the voxelized space, we project the classified point clouds into the voxels and classify the voxels into five types, including:

1. Voxels containing building points only are defined as building voxels. A LOS stops immediately upon encountering them. They are used to extract building boundaries.
2. Voxels containing grass points without building points are defined as grass voxels. A LOS stops immediately upon encountering them, and they are used in green visibility calculation.
3. Voxels containing ground points without building or grass points are defined as ground voxels. A LOS stops immediately upon encountering them and they do not contribute to green visibility.
4. Voxels containing only tree points are defined as tree voxels. Their penetration probability is later calculated according to the point cloud density within the voxel. When a LOS encounters them, the intensity attenuation is determined probabilistically.
5. If a voxel contains no points of any type, it is defined as an empty voxel.

According to the voxel classification rules, if a voxel contains at least one building point, it is classified as a building voxel. Therefore, for building façade completion, the translation distance only needs to be less than or equal to the voxel size, *i.e.*, 1m. The voxelized study area and its comparison with the real-world terrain are shown in Figure 5:

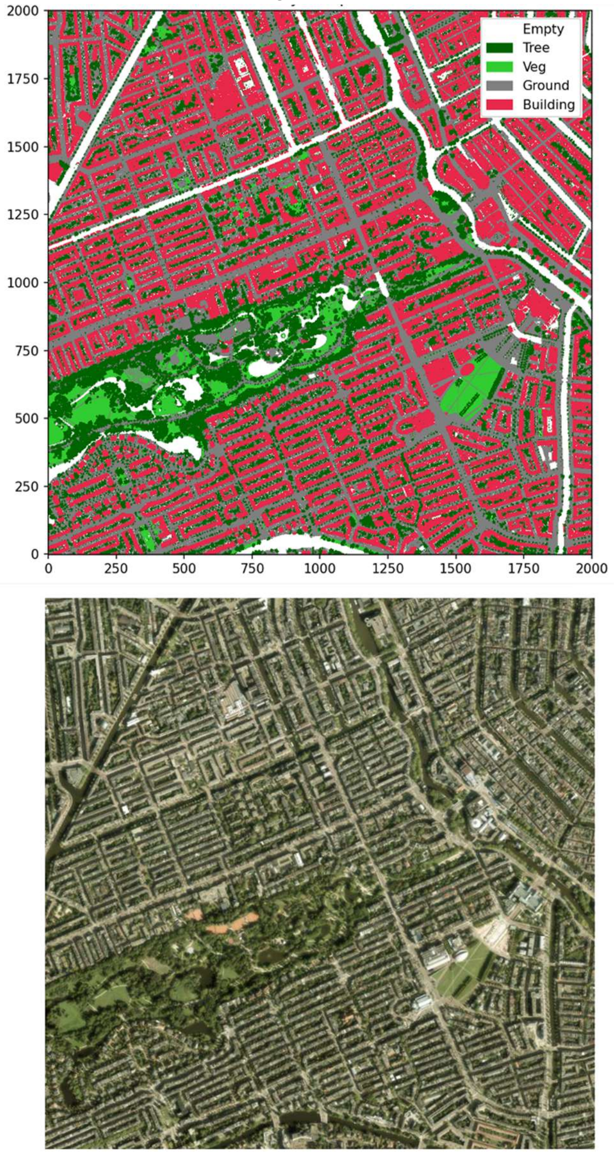

Figure 5. Voxelized area and corresponding real-world scene.

2.3 Viewpoints and LOS Sampling

At the beginning of each calculation, a height layer is first selected, and the voxels corresponding to that layer are extracted. The calculation is then carried out using the empty voxels in that layer. We select only empty voxels as possible observation points in order to simulate the actual visual accessibility of observers in urban space. This design excludes occupied regions such as buildings and tree trunks, ensuring that the analysis is consistent with human behavior.

Some street-view studies set the viewpoint height at 1.3 m (Tang et al., 2023). Therefore, based on existing studies and the characteristics of this experiment, we set the midpoint of the voxel corresponding to a near first-floor eye-level position, namely an absolute height of 2.5 m, as the first-floor viewpoint height. We set 3m as the height of each floor, then sample viewpoints from the first to the tenth floor.

For the calculation at a given floor, the geometric center of each empty voxel is used as the center of a sphere, and 150 rays are generated in all directions using the Fibonacci sphere sampling method to simulate the LOS of a person looking around, as shown in Figure 6. In high-density areas, the travel distance of LOS is generally limited, so a maximum viewing distance of 200 m is sufficient for our needs. Each LOS is sampled every 1 m as it moves forward, ensuring that every voxel passed through by each LOS can be calculated. The number of LOS, the maximum viewing distance, and the sampling step length can all be adjusted according to the dataset and experimental settings.

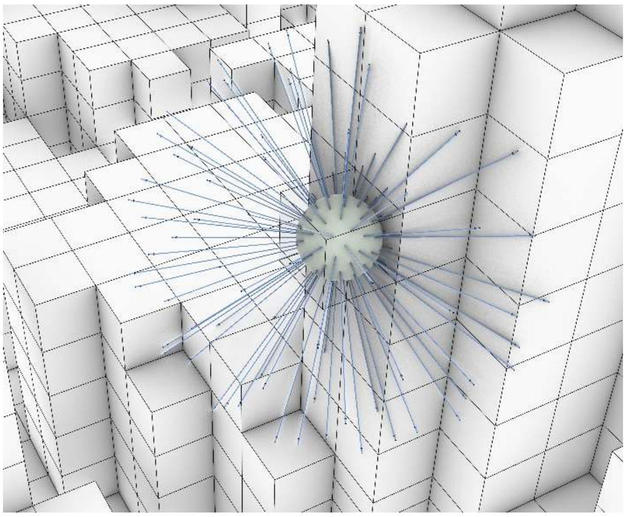

Figure 6. Schematic of LOS generation(blue lines represent the LOS).

2.4 Penetration Probability Model

Unlike traditional studies based on 2D images or 3D white models, in this experiment the LOS intensity influences its travel distance and GVI. Therefore, when a LOS encounters a tree voxel, it does not stop immediately. Instead, its intensity is attenuated according to a certain rule, and it may continue to move forward until its intensity drops to zero. This allows a more realistic simulation of the semi-transparent occlusion effect of leaves.

Specifically, before calculating GVI, we first traverse all tree voxels in the study area and count their point cloud contents to determine the critical value of voxel point cloud density. We define voxel point cloud density as the ratio between the number of points within a voxel and the voxel volume. The point cloud density is calculated in Equation (1):

$$\rho = \frac{n}{l^3}, \tag{1}$$

where n = the number of points within the voxel
l = voxel size

The value of voxel point cloud density ρ_{max} is the threshold that distinguishes attenuation from full blockage. If the density is below ρ_{max}, the LOS intensity is attenuated according to the voxel point cloud density; while if the density is greater than or equal to ρ_{max}, the LOS is stopped directly.

In the preliminary experiment, we traversed and extracted the point cloud characteristics of all tree voxels in the study area, as shown in Figure 7, and found that the distribution is right-skewed with a long tail. The mean ρ is 4.69, the median is 3, and the 90th percentile value is 10. To exclude the influence of extreme values and to keep it physically reasonable, we set the ρ_{max} to 10. Since the voxel size is 1m, this means that when the number of points in a tree voxel is $n \geqslant 10$, the foliage is considered too dense for the LOS to penetrate. When n<10, the LOS attenuates according to the Beer–Lambert law (Casasanta et al., 2022) and the specified attenuation coefficient. The attenuation of the LOS is calculated in Equation (2):

$$\begin{cases} p = 0, \ \mathrm{n} \geq \mathrm{n}_{max} \\ e^{-\alpha \times p}, \ 0 < \mathrm{n} < \mathrm{n}_{max}, \\ p = 1, \ \mathrm{n} = 0 \end{cases} \tag{2}$$

where p = the penetration probability of the LOS
α = the attenuation coefficient

Based on n_{max} ,we set $\alpha = 0.25$, that means when a tree voxel contains 1 point, the penetration probability is 0.78, and 0.47 for 3 points, satisfying the process in which p smoothly decays to near 0 as the number of points increases from 1 to 10.

Penetration probability directly affects the final GVI and SOP. As one of the distinctive features of our method compared with others, this will be further explained in the experimental results.

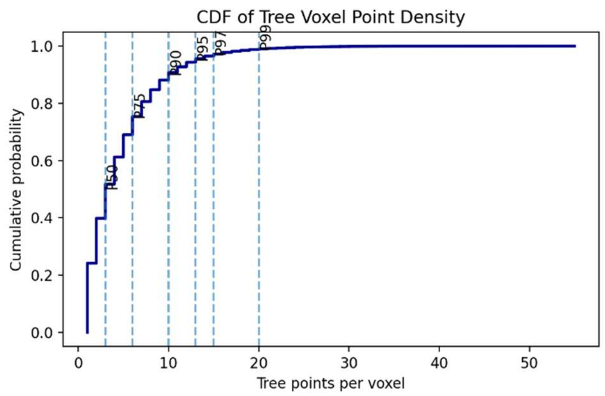

Figure 7. Distribution characteristics of tree point counts in the study area.

2.5 Calculation of GVI and SOP

One of the main outputs of our calculation is the stratified spatial distribution map of GVI. For a single LOS, the energy absorbed by vegetation during its forward movement is calculated as the score of that LOS, denoted as *GV*, as shown in Equation (3):

$$GV = \sum_{i=1}^{S} \left(T_{r,i} \times (1 - p_{r,i}) \times G_{r,i} \right), \tag{3}$$

where $p_{r,i}$ = penetration probability at the i-th step
$T_{r,i}$ = remaining energy of the LOS before the i-th step
S = the whole step before the LOS stops

$G_{r,I}$ is an indicator function. If the voxel is a tree or grass voxel, then G=1; while if it is a building or ground voxel, then G=0. For example, supposing a LOS has an initial intensity of 1. When it passes through the first tree voxel, the penetration probability is 0.4, so the LOS intensity after passing through it becomes 0.6. The second one is a building voxel and the LOS stops. The final GV of this LOS is 0.4, meaning that 40% of this LOS reach foliage, and after passing through it, 60% of it reach the solid building.

For a given empty voxel, the average absorbed energy values of all LOS are calculated as the GVI of that voxel location. By assigning the GVI to all analyzed voxels in a given height layer, the GVI spatial distribution map of that layer is formed. This result reflects the overall GVI at a given location in the city, as shown in Equation (4):

$$GVI = \frac{1}{R} \sum_{r=1}^{R} (\mathrm{G}V), \tag{4}$$

where R = the total number of LOS generated by the voxel

Supposing that among 100 LOS generated by a voxel, 45 hit tree or grass voxels. In some methods, the GVI of this location might be recorded as 0.45. In our method, however, 55 of these 100 LOS would have a score of 0, while the remaining 45 would each have a score between 0 and 1. The final GVI is the average of these 100 values.

This calculation also produces stratified SOP distribution maps. For a single LOS, the equivalent travel distance under the influence of penetration probability is calculated as the penetration distance *OP*, as shown in Equation (5):

$$OP = \sum_{i=1}^{S} \left(T_{r,i} \times p_{r,i} \right), \tag{5}$$

where $p_{r,i}$ = penetration probability at the i-th step
$T_{r,i}$ = remaining energy of the LOS before the i-th step
S = the whole step before the LOS stops

Their product represents the penetration distance contributed by that step. For a given empty voxel, the average penetration distance of all LOS is calculated as the mean penetration distance at that voxel location, and then divided by the maximum viewing distance for normalization to obtain openness *SOP*, as shown in Equation (6):

$$SOP = \frac{1}{R \times S} \sum_{r=1}^{R} (\mathrm{O}P), \tag{6}$$

where R = the total number of LOS generated by the voxel

This indicator can reflect the degree of enclosure and openness of urban space. For example, if a LOS advances for 20 steps in total, and at the 10th step its intensity is attenuated to 50% by leaf occlusion, then its OP is 9+1×0.5+10×0.5=14.5 steps. Compared with traditional binary collision models, this method more realistically reflects visual penetration depth in the presence of semi-transparent vegetation occlusion. Combined with the GVI spatial distribution map, it can help identify certain special spaces, for example, high GVI but low SOP may indicate dense trees planted close to windows.

We also can generate specific analytical maps based on the above results, such as the distribution map of the height at which GVI first exceeds 0.3 for a given XY location, or the height at which GVI reaches its maximum.

2.6 LOS Tracing Process

Each LOS has a predetermined forward direction when generated. The initial intensity is 1, and the LOS advances along the specified direction. Sampling is performed at every step as it moves forward, and at each sampling point the voxel in which the current endpoint of the LOS is used for evaluation. At each sampling step, the LOS determines the type of encountering voxel. If it is a grass, building, or ground voxel, the LOS stops immediately, simulating the effect of solid obstacles. If it is a tree voxel, the point cloud density is used to determine whether the LOS stops. If not, the amount of intensity attenuation; while if it is an empty voxel, the LOS continues to move forward. When a LOS stops because it hits an obstacle or reaches the maximum viewing distance, its forward path is then evaluated. When it has encountered any tree voxels, or it stops upon hitting a grass voxel, then GV is scored; otherwise, it is recorded as not seeing greenery and receives a score of 0.

We use several possible LOS and their movement processes as examples to explain the main process of the calculation. As shown in Figure 8, three LOS are generated from an empty voxel at a height of 8.5m, and the three LOS lie in the same XZ plane. The first LOS *r1* moves parallel to the horizontal plane, the second LOS *r2* moves downward at an angle of 30° to the horizontal plane, and the third LOS *r3* moves upward at an angle of 45° to the horizontal plane. In this case, the maximum viewing distance is set to 200 m, the sampling step length is 1m, and the number of sampling steps is 200. There is a tree at a horizontal distance of 6m from the viewpoint.

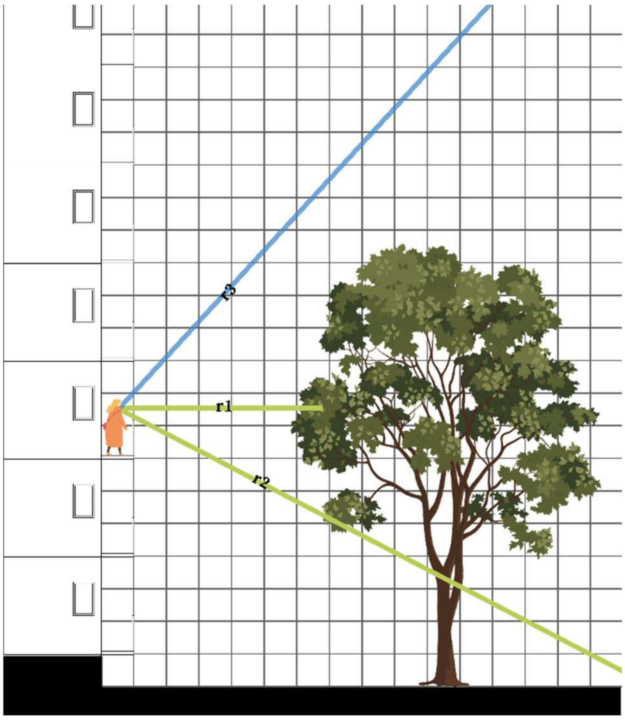

Figure 8. Schematic of LOS.

First, LOS *r1* moves horizontally. During the first five steps, it passes only through empty voxels, and its energy remains 1, that is, $T_{r1,5} = 1$, $P = 1$. At the sixth step, it encounters a tree voxel, but this voxel is relatively sparse, containing only 3 tree points, which is lower than the $\rho_{\max}$ of 10. Therefore, the LOS does not stop, but its intensity attenuates. The penetration probability $P_{r1,6}$ is approximately 0.472, which means that the voxel consumes 0.528 of the LOS energy. At this point, the $T_{r1,7}$ is 0.472, and it can continue to move forward. At the seventh step, it again encounters a voxel of the same tree, but this voxel contains 12 tree points, exceeding the threshold of 10. Therefore, the LOS stops at this step, and the voxel consumes 0.472 of the LOS energy. The final score is GV_{r1} = 0.472+0.528 = 1, and the OP_{r1} is 0.027.

LOS *r2* passes only through empty voxels during the first six steps, and its energy remains 1, that is, $T_{r2,6} = 1$, $P = 1$. At the seventh step, the sampled voxel is a tree voxel with 5 tree points, which is lower than the $\rho_{\max}$ of 10. Therefore, the LOS does not stop, but its intensity attenuates, and the penetration probability is $P_{r2,7} = 0.286$. It then hits the ground at the seventeenth step, without encountering any other non-empty voxels during the interval. At this point, the LOS stops. This LOS is counted as seeing greenery, with GV_{r2} =0.714 and OP_{r2} = 0.044.

LOS *r3* does not encounter any non-empty voxel until it reaches the maximum viewing distance. Its GV_{r3} is 0, but its OP_{r3} is 1.

3. Experimental Results

We conducted an experiment and successfully obtained the distribution of GVI and SOP in the study area from the height layer of 2.5m to 29.5m. as shown in Figure 9 and 10:

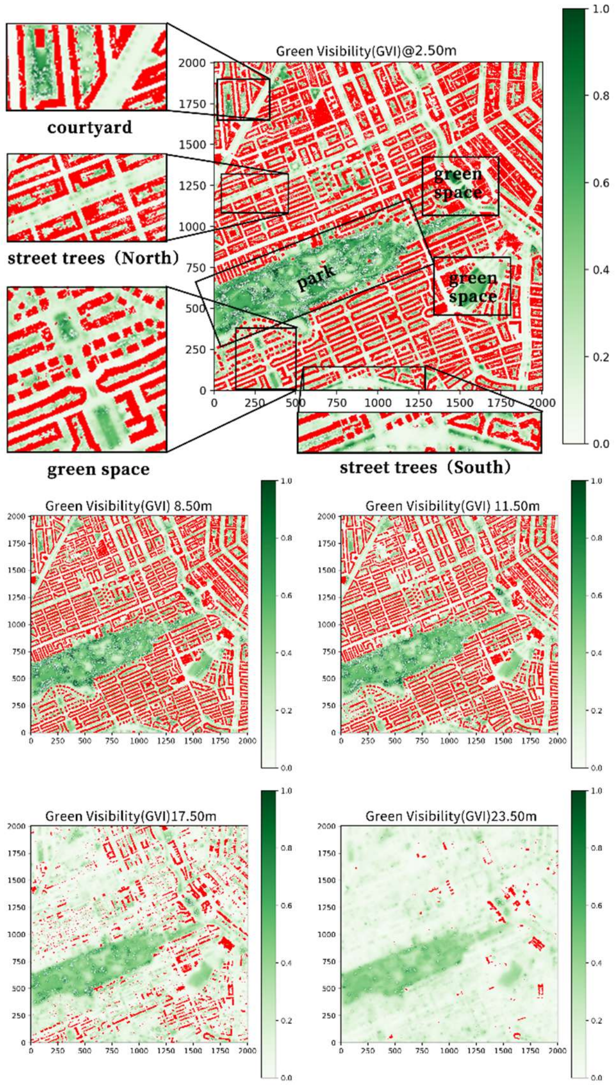

Figure 9. Results of Green visibility Index (GVI). The red areas represent the building voxels at each height layer, the green areas represent the GVI values at each voxel location.

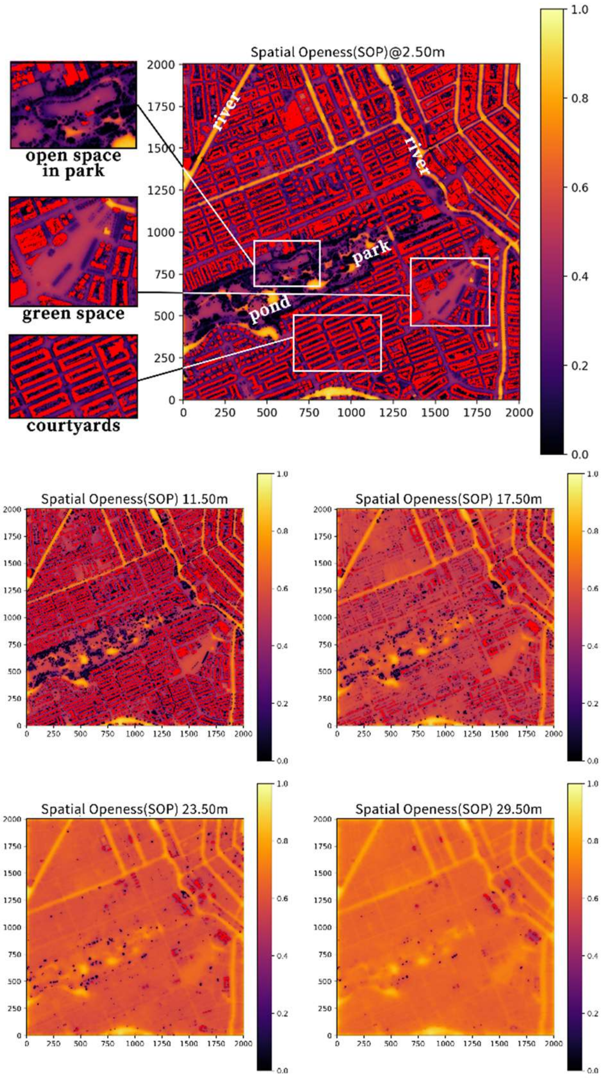

Figure 10. Spatial openness (SOP). The red areas represent the building voxels at each height layer, the colors ranging from black to yellow represent the SOP values at each location.

3.1 Spatial Distribution Characteristics of GVI

In the horizontal dimension, GVI mainly attains high values around parks and small green spaces, and relatively high values are also found in some enclosed residential courtyards (see Figure 9). This is consistent with our expectations, as these areas are not only close to greenery but also contain concentrated vegetation. Meanwhile, the GVI around some street trees in the north is relatively low (Figure 9), possibly because their sparse distribution results in a lower proportion of green-view LOS within a single voxel.

In the vertical dimension, the overall GVI tends to decrease with height, while the differences among regions gradually diminish as height increases. Specifically, the areas around some street trees in the south decline rapidly in Figure 9, some of them show a prominent advantage at 2.5 m, but by 11.5 m they are already close to the median value. Even though the GVI distribution becomes more moderate at higher levels, the parks and green spaces can still be clearly identified, indicating their contribution to GVI.

3.2 Spatial Distribution Characteristics of SOP

Because of the limitation of the Lidar dataset, data are missing for rivers and park ponds, LOS in these areas can produce extremely high openness values, so they need to be excluded in our explanation.

On this basis, in the horizontal dimension, SOP attains high values in large green spaces and open parts of parks, while its values are low inside enclosed courtyards. In the vertical dimension, it shows an overall increasing trend, and the differences among regions likewise tend to decrease.

3.3 Combined Analysis of GVI and SOP

Although the areas around buildings near parks and the interior spaces of enclosed courtyards have relatively high GVI, their SOP is quite low, which is a typical manifestation of vegetation planted very close to windows. In contrast, the areas around the public green space in the southeast have both high GVI and high SOP, because they contain large lawns and relatively fewer trees. Since the streets in the study area have similar widths and vegetation is generally planted inside the courtyards, there are no obvious spaces with both low GVI and low SOP. Results are shown in Figure 11:

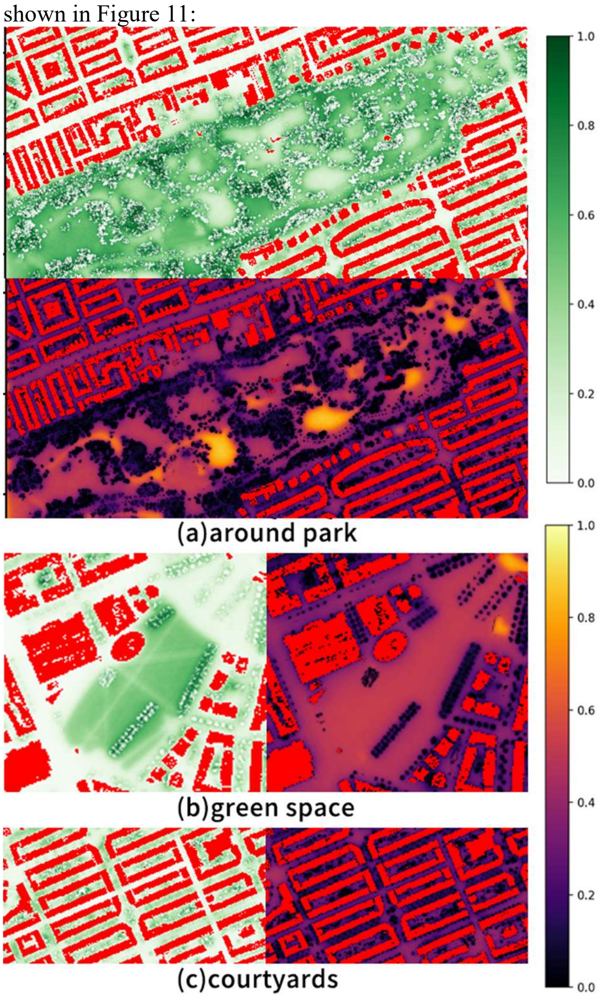

Figure 11. Combined Analysis of GVI and SOP (2.5m). (a) shows the comparison between GVI and SOP around parks, (b) around open green spaces, and (c) within some courtyards.

3.4 Other Related Analyses

We plotted the distribution map of the height at which the normalized GVI and SOP reach their maximum values, as shown in Figure 12:

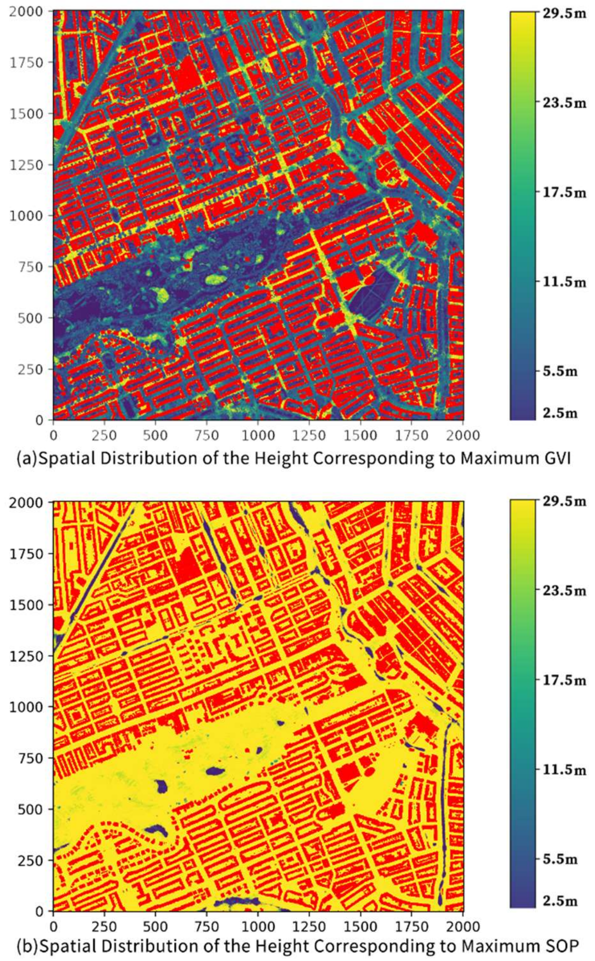

Figure 12. The height at which GVI and SOP reach their maximum at each place. The red areas represent the building voxels, the colors ranging from blue to yellow represent the heights at which the statistics of the places reach their maximum.

Figure 12 (a) shows the height at which GVI reaches its maximum at each place. Within the calculated height range of 2.5–29.5 m, the maximum value may occur at an intermediate height if the value first increases and then decreases, or at top height (29.5 m) if it does not decrease within this range.

Figure 12 (b) shows the height at which SOP reaches its maximum at each place. Except for some areas without data (blue places), SOP generally reaches its maximum at the top height 29.5m (yellow places). This is consistent with the fact that the higher the viewpoint, the more open the space tends to be.

4. Conclusion

This study constructs a 3D stratified GVI analysis framework for urban space at the city scale. Based on lightly semantically labeled point cloud information, the framework can achieve a true 3D simulation of GVI in urban space under conditions of limited precision, and can compare the differences in visual environments at different locations across multiple height layers. By introducing a voxel-level penetration probability model to simulate the occlusion effect of semi-transparent tree canopies on LOS, they no longer simply stop when passing through trees, but instead attenuate in intensity according to tree point cloud density. Based on this, we further construct the calculation methods of *green visibility GVI* and *spatial openness SOP*, so that the two complementary dimensions can depict how much greenery can be seen and how far LOS can penetrate within the proposed framework. The voxel model is not only an important carrier for the quantification of urban green visibility, but can also be seamlessly connected in the future with multidisciplinary applications such as urban microclimate simulation and digital twin city construction (Xu et al., 2024).

Experimental results based on the AHN5 airborne point cloud data show that, in the horizontal dimension, GVI in the study area mainly attains high values around parks, green spaces, and some enclosed courtyards; while areas around street trees make some contribution but remain relatively limited overall. In the vertical dimension, GVI generally decreases with increasing height, and the differences among regions gradually shorten.

In the horizontal dimension, SOP mainly reaches high values in open green areas, main roads, and larger open spaces, while it is low in enclosed courtyards and locally strongly obstructed areas. In the vertical dimension, it shows an overall increasing trend and likewise exhibits a reduction in spatial differentiation as height increases. In other words, in high-density urban residential environments, GVI and SOP do not change synchronously. As higher space usually becomes more open, but not necessarily greener in visual perception.

This study also contains some limitations. For instance, the parameters related to penetration probability may lack support of real-world tests. In addition, the calculation of GVI is relatively simple, and the dataset has not been fully utilized via other factors such as the distance effects of trees and grass. In the future, we will improve the relevant parameters and the computational framework, introduce more variables, combine seasonal or tree-species simulations, and promote the integration of multiple data sources including street-view data, so as to further enhance the value of this framework in urban design, residential evaluation, and refined urban governance.

Acknowledgements

This research was Sponsored by Natural Science Foundation of Shanghai (grant number: 24ZR1469300).

References

AHN, 2023. Home [Landingspagina]. https://www.ahn.nl/ (accessed 11 March 2026).

Aleksandrov, M., S. Zlatanova, L. Kimmel, J. Barton, and B. Gorte, 2019, Voxel-based visibility analysis for safety assessment of urban environments, *ISPRS Ann. Photogramm. Remote Sens. Spatial Inf. Sci., IV-4/W8*, 11–17, 2019, https://doi.org/10.5194/isprs-annals-IV-4-W8-11-2019

Aljumaily, H., Laefer, D.F., Cuadra, D., Velasco, M., 2023. Point cloud voxel classification of aerial urban LiDAR using voxel attributes and random forest approach. *International Journal of Applied Earth Observation and Geoinformation*, 118, 103208. doi.org/10.1016/j.jag.2023.103208.

Casasanta, G., Falcini, F., Garra, R., 2022. Beer–Lambert law in photochemistry: a new approach. *Journal of Photochemistry and Photobiology A: Chemistry*, 432, 114086. doi.org/10.1016/j.jphotochem.2022.114086.

Feng, Y., Yang, F., 2023. Developing a voxel-based sightline sampling algorithm for calculating panoramic visible green index. *International Archives of the Photogrammetry, Remote Sensing and Spatial Information Sciences*, XLIV-4/W1, 123-130. doi.org/10.5194/isprs-archives-XLIV-4-W1-123-2023.

Huang, S., Liu, L., Fu, X., Dong, J., Huang, F., Lang, P., 2022. Overview of LiDAR point cloud target detection methods based on deep learning. *Sensor Review*, 42(5), 485-502. doi.org/10.1108/SR-01-2022-0022.

Jia, J. S. Zlatanova, H. Liu, M. Aleksandrov, K. Zhang, 2023, A design-support framework to assess urban green spaces for human wellbeing, *Sustainable Cities and Societies*, Vol 98, Nov. 2023, 104779

Ki, D., Lee, S., 2021. Analyzing the effects of green view index of neighborhood streets on walking time using Google Street View and deep learning. *Landscape and Urban Planning*, 205, 103920. doi.org/10.1016/j.landurbplan.2020.103920.

Kumakoshi, Y., Chan, S.Y., Koizumi, H., Li, X., Yoshimura, Y., 2020. Standardized green view index and quantification of different metrics of urban green vegetation. *Sustainability*, 12(18), 7434. doi.org/10.3390/su12187434.

Li, J., S. Zlatanova and R. Stouffs, 2025, Cooling effects of urban green spaces: A systematic review of methods applied in the past two decades, *Sustainable Cities and Society*, Vol. 133, 1 October 2025, 106833

Tang, L., He, J., Peng, W., Huang, H., Chen, C., Yu, C., 2023. Assessing the visibility of urban greenery using MLS LiDAR data. *Landscape and Urban Planning*, 232, 104662. doi.org/10.1016/j.landurbplan.2022.104662.

Wang, Y., Zlatanova, S., Yan, J., Huang, Z., Cheng, Y., 2021. Exploring the relationship between spatial morphology characteristics and scenic beauty preference of landscape open space unit by using point cloud data. *Environment and Planning B: Urban Analytics and City Science*, 48(7), 1822-1840. doi.org/10.1177/2399808320949885.

Wang, Y, Y. Cheng, S. Zlatanova, S. Cheng, 2024, Quantitative Analysis Method of the Organizational Characteristics and Typical Types of Landscape Spatial Sequences Applied with a 3D Point Cloud Model, *Land* 13 (6), 770 https://doi.org/10.3390/land13060770

Wu, B., Yu, B., Shu, S., Liang, H., Zhao, Y., Wu, J., 2021. Mapping fine-scale visual quality distribution inside urban streets using mobile LiDAR data. *Building and Environment*, 206, 108323. doi.org/10.1016/j.buildenv.2021.108323.

Xia, T., Zhao, B., Xian, Z., Zhang, J., 2023. How to systematically evaluate the greenspace exposure of residential communities? A 3-D novel perspective using UAV photogrammetry. *Remote Sensing*, 15(6), 1543. doi.org/10.3390/rs15061543.

Xu, H., Wang, C.C., Shen, X., Zlatanova, S., Paolini, R., 2024. Refined definition of level-of-detail for tree models in support of microclimate simulation. SSRN. doi.org/10.2139/ssrn.4882313.

Yang, J., Zhao, L., McBride, J., Gong, P., 2009. Can you see green? Assessing the visibility of urban forests in cities. *Landscape and Urban Planning*, 91(2), 97-104. doi.org/10.1016/j.landurbplan.2008.12.004.

Yu, S., Yu, B., Song, W., Wu, B., Zhou, J., Huang, Y., Wu, J., Zhao, F., Mao, W., 2016. View-based greenery: a three-dimensional assessment of city buildings' green visibility using floor green view index. *Landscape and Urban Planning*, 152, 13-26. doi.org/10.1016/j.landurbplan.2016.04.004.

Zhang, H., Wang, C., Tian, S., Lu, B., Zhang, L., Ning, X., Bai, X., 2023. Deep learning-based 3D point cloud classification: a systematic survey and outlook. *Displays*, 79, 102456. doi.org/10.1016/j.displa.2023.102456.

Xu, H., Wang, C. C., Shen, X., & Zlatanova, S., 2021. 3D tree reconstruction in support of urban microclimate simulation: A comprehensive literature review. *Buildings*, 11(9), 417. https://doi.org/10.3390/buildings11090417